

# EUROPEAN ORGANIZATION FOR NUCLEAR RESEARCH

## Proposal to the ISOLDE and Neutron Time-of-Flight Committee

### Evolution of quadrupole and octupole collectivity north-east of $^{132}\text{Sn}$ : the even $^{140,144}\text{Xe}$ isotopes

12 May 2021

C. Henrich<sup>1</sup>, Th. Kröll<sup>1</sup>, A.-L. Hartig<sup>1</sup>, I. Homm<sup>1</sup>, H.-B. Rhee<sup>1</sup>, M. Rudigier<sup>1</sup>, C. Sürder<sup>1</sup>, M. von Tresckow<sup>1</sup>, L. Atar<sup>1</sup>, M. Scheck<sup>17</sup>, P. Reiter<sup>2</sup>, M. Droste<sup>2</sup>, K. Arnsward<sup>2</sup>, A. Blazhev<sup>2</sup>, H. Hess<sup>2</sup>, H. Kleis<sup>2</sup>, N. Warr<sup>2</sup>, C. Berger<sup>3</sup>, C. Berner<sup>3</sup>, V. Bildstein<sup>5</sup>, J. Cederkäll<sup>6</sup>, D. Cox<sup>6</sup>, G. de Angelis<sup>8</sup>, H. De Witte<sup>9</sup>, L. Gaffney<sup>4</sup>, R. Lozeva<sup>12</sup>, G. Georgiev<sup>12</sup>, K. Stoychev<sup>12</sup>, R. Gernhäuser<sup>3</sup>, A. Illana Sisón<sup>7</sup>, M. Matejska-Minda<sup>13</sup>, P. J. Napiorkowski<sup>13</sup>, K. Wrzosek-Lipska<sup>13</sup>, K. Hadyńska-Klęk<sup>13</sup>, M. Komorowska<sup>13</sup>, J. Ojala<sup>7</sup>, J. Pakarinen<sup>7</sup>, G. Rainovski<sup>14</sup>, D. Kocheva<sup>14</sup>, K. Gladnishi<sup>14</sup>, L. Werner<sup>3</sup>, M. Zielińska<sup>11</sup>, W. Korten<sup>11</sup>, D. Kalaydjieva<sup>11</sup>, K. Wimmer<sup>16</sup>, A. Stuchbery<sup>15</sup>, B. Olaizola<sup>10</sup>, P. Spagnoletti<sup>18</sup>, J. Allmond<sup>19</sup>, P. Thirolf<sup>20</sup>, L. M. Fraile<sup>21</sup>, and the MINI-BALL and HIE-ISOLDE collaborations

<sup>1</sup>TU Darmstadt, Germany; <sup>2</sup>University of Cologne, Germany; <sup>3</sup>TU München, Germany; <sup>4</sup>University of Liverpool, United Kingdom; <sup>5</sup>University of Guelph, Canada; <sup>6</sup>Lund University, Sweden; <sup>7</sup>University of Jyväskylä, Finland; <sup>8</sup>INFN LNL, Italy; <sup>9</sup>KU Leuven, Belgium; <sup>10</sup>CERN-ISOLDE, Switzerland; <sup>11</sup>CEA Saclay, France; <sup>12</sup>IJCLab, Orsay, France; <sup>13</sup>HIL, University of Warsaw, Poland; <sup>14</sup>SU Sofia, Bulgaria; <sup>15</sup>ANU, Canberra, Australia; <sup>16</sup>CSIC Madrid, Spain; <sup>17</sup>UWS, Paisley, United Kingdom; <sup>18</sup>SFU, Burnaby, Canada; <sup>19</sup>ORNL, Oak Ridge, USA; <sup>20</sup>LMU, München, Germany; <sup>21</sup>UCM, Madrid, Spain

**Spokespersons:** C. Henrich [chenrich@ikp.tu-darmstadt.de], Th. Kröll [tkroell@ikp.tu-darmstadt.de]

**Contact person:** B. Olaizola [Bruno.Olaizola@cern.ch]

**Abstract:** We propose to study excited states in even Xe isotopes north-east of the doubly-magic  $^{132}\text{Sn}$  by  $\gamma$ -ray spectroscopy following “safe” Coulomb excitation. The experiment aims to determine  $B(E2)$ ,  $Q_2$ , and  $B(E3)$  values to follow the evolution of quadrupole and octupole collectivity when going away from the shell closures at  $Z = 50$  and  $N = 82$ . In a first experimental campaign in 2016 (IS548), the isotope  $^{142}\text{Xe}$  has been measured with the MINIBALL & C-REX set-up. We propose to extend these studies to  $^{140,144}\text{Xe}$  in order to obtain a systematic view on the collectivity of even Xe isotopes going away from  $N = 82$  towards  $N = 90$ .



# 1 Motivation

The region around the doubly-magic nucleus  $^{132}\text{Sn}$  is the focus of many efforts in both experimental and theoretical nuclear physics. Since the astrophysical  $r$  process is expected to pass through this region, the understanding of the nuclear structure has also an impact on the description of the  $A \approx 130$  peak in the solar element abundances<sup>1</sup>.

Unlike the neighbouring even Te isotopes ( $Z = 52$ ), the studies of the even Xe isotopes ( $Z = 54$ ) have revealed a very regular behaviour. The  $B(E2, 0_{\text{gs}}^+ \rightarrow 2_1^+)$  values are symmetric with respect to a minimum at the  $N = 82$  shell closure and the trend at higher neutron-rich numbers is well reproduced by a simple Grodzins-type systematics as well as by shell-model calculations. The experimental results before HIE-ISOLDE came from Coulomb excitation at REX-ISOLDE. But only  $B(E2, 0_{\text{gs}}^+ \rightarrow 2_1^+)$  and, for most cases,  $B(E2, 2_1^+ \rightarrow 4_1^+)$  values were determined [2, 3]. Complementary results came from direct lifetime measurements [4, 5] for the same states, but  $^{144}\text{Xe}$  was not reached.

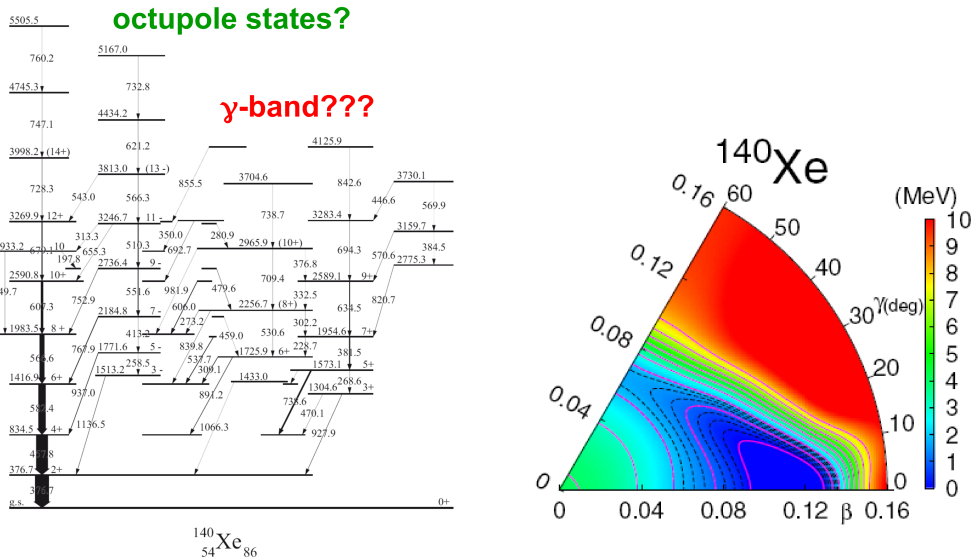


Figure 1:  $^{140}\text{Xe}$ : known level scheme [7] (left), potential energy surface [9] (right).

For the isotope  $^{140}\text{Xe}$  the most extended level scheme is based on prompt spectroscopy of fission fragments from the spontaneous fission of  $^{248}\text{Cm}$  [6, 7] and more recently of  $^{252}\text{Cf}$  [8]. It exhibits states with both positive and negative parity (Fig. 1, left). In addition to the yrast band, low-lying states are candidates for members of a  $\gamma$ -band, the first in this region [7]. This is supported by CHFSM calculations predicting some  $\gamma$ -softness for this nucleus [9] (Fig. 1, right). The triaxiality has also a potential impact on nuclear astrophysics [10]. Applying the “Kumar-Cline sum rule” [11, 12] conclusions on the nuclear shape and the vibrational or rotational nature of the excitations can be drawn. The negative-parity states are interpreted as candidates of an octupole band allowing to investigate the emergence of octupole collectivity in this region.

**However, no  $B(E2)$  or  $B(E3)$  values for the side bands in  $^{140}\text{Xe}$  are experimentally known.**

<sup>1</sup>In 2017, for the first time observations confirmed a binary neutron star merger as an astrophysical site of the  $r$ -process with the light curves as indicator for the isotopes produced and their decay [1].

Going more exotic,  $^{142}\text{Xe}$  has with  $N = 88$  a so-called “magic” octupole number. For  $Z = 56$  and  $N = 88$ , hence  $^{144}\text{Ba}$ , the octupole correlations are expected to be strongest. A recently published large  $B(E3)$  value for this nucleus, although with large error, seems to support this [13].  $^{142,144}\text{Ba}$  have been investigated at HIE-ISOLDE too, the analysis is ongoing [14].

Profiting from the higher beam energies available at HIE-ISOLDE, the use of a high- $Z$  target, and employing the C-REX Si array with a large solid angle coverage,  $^{142}\text{Xe}$  has been investigated in experiment IS548 [15, 16, 17, 18, 19].

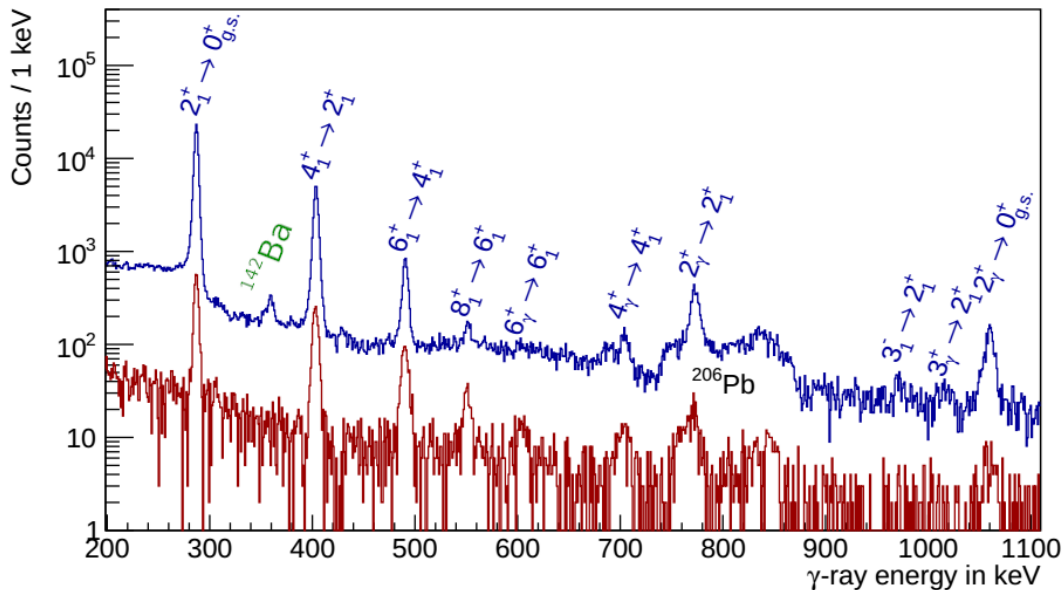


Figure 2: IS548:  $\gamma$ -ray energy-spectra Doppler corrected with respect to  $^{142}\text{Xe}$ . Particles detected in forward direction (blue) and in backward direction, barrel only (red) [19].

Fig. 2 shows a Doppler corrected  $\gamma$ -ray spectrum for  $^{142}\text{Xe}$  (about 10.5 shifts). Most of the statistics are  $\gamma$  rays in coincidence with a particle in the forward CD of C-REX. The backward hemisphere of C-REX added only few statistics on an absolute scale, but the relative intensities allowed for a better analysis of multiple-step excitation which was very important because the level scheme of  $^{142}\text{Xe}$  was not known very well. E.g., the intensity ratio  $Y(8_1^+ \rightarrow 6_1^+)/Y(2_\gamma^+ \rightarrow 0_{gs}^+)$  clearly shows that the  $8_1^+$  state is excited by multiple-step excitation whereas the  $2_\gamma^+$  state is populated dominantly by single-step excitation. In fact, also the information from decay data taken at RIKEN [20] was very helpful to confirm the level scheme constructed from our data based on  $\gamma$ - $\gamma$  coincidences and excitation probability as function of the scattering angle.

In short, the most important results for  $^{142}\text{Xe}$  [18]:

- The first  $3^-$  could be confirmed (assigned in prompt spectroscopy of fission fragments from the spontaneous fission of  $^{248}\text{Cm}$  Ref. [6]). Because of the low statistics, the  $B(E3)$  value has a large uncertainty (about 100%), but rather confirms a small value consistent with Raman’s formula [21] than enhanced octupole collectivity.
- $B(E2)$  values have been determined within the ground state band up to the  $B(E2, 8^+ \rightarrow 6^+)$  (uncertainties about 17-26%). For the  $B(E2, 4^+ \rightarrow 2^+)$  an inconsistency with the result from the lifetime measurement [5] has been found.

- Quadrupole moments  $Q_2$  have been extracted for the  $2^+$ ,  $4^+$ ,  $6^+$  states. However, the extracted values are small and have large errors (about 50%-100%).
- For the first time, a  $\gamma$  band - tentative spin-parity assignments for the members ( $2_\gamma^+$ ), ( $3_\gamma^+$ ), ( $4_\gamma^+$ ) and ( $6_\gamma^+$ ) - has been observed in this isotope. For the ( $2_\gamma^+$ ) state two  $B(E2)$  values connecting this state to the ground state band could be measured (uncertainties about 50% and 100%).

The quadrupole collectivity is well reproduced by new large-scale shell model [22] and beyond-mean field calculations [23] motivated by our new findings. A publication with the results is in preparation.

Various approaches have been used to generate shell-model interactions capable of predicting the behaviour of neutron-rich nuclei beyond  $N = 82$  using either empirical approaches (e.g. SMPN) [24] or realistic free nucleon-nucleon potentials (e.g. CD-Bonn), renormalized by either G-matrix (e.g. CWG) [25] or  $V_{low k}$  methods [26]. For Sn isotopes, the calculations with empirical interactions predict even a new shell closure at  $N = 90$  as the  $\nu f_{7/2}$  orbital is filled, whereas the calculations with realistic interactions do not find such

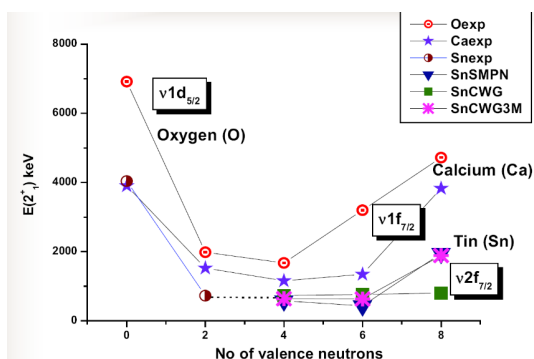


Figure 3: Phenomenological and realistic predictions towards  $N = 90$  for the Sn isotopic chain

an effect. The  $\nu f_{7/2}$  orbit being filled beyond  $N = 82$  has an interesting analogy with the Ca isotopic chain where a  $\nu f_{7/2}$  orbital is filled between  $N = 20$  and  $N = 28$ . There was the long-standing problem that realistic interactions were not able to reproduce the shell closure at  $N = 28$ . This has been resolved very recently by including three-body forces [27]. Indeed, including three-body forces a shell closure at  $N = 90$  occurring in  $^{140}\text{Sn}$  is predicted also by calculations based on realistic interactions (CWG3M) [28]. The  $^{140}\text{Sn}$  and  $^{142}\text{Te}$  isotopes at  $N = 90$  are currently out of reach for in-beam studies (and decay studies as well) and  $^{144}\text{Xe}$  is the closest isotope to  $^{140}\text{Sn}$  that experimentally can be reached. The only experimental  $B(E2, 0_{\text{gs}}^+ \rightarrow 2_1^+)$  value from REX-ISOLDE [2] is similar to that in  $^{142}\text{Xe}$  which may indicate a flattening of the increase of  $B(E2)$  values going away from  $N = 82$ , but the 50% statistical uncertainty<sup>2</sup> prevents any firm conclusion. Better knowledge on the  $B(E2)$  values is essential to verify or falsify effects appearing at  $N = 90$ .

**However, no  $B(E2)$  values for  $^{144}\text{Xe}$  with uncertainties allowing for conclusions on structural effects at  $N = 90$  are experimentally known.**

## 2 Proposed experiment, method and setup

We propose to extend our study of quadrupole and octupole collectivity of neutron-rich Xe isotopes by safe Coulomb excitation at HIE-ISOLDE started with  $^{142}\text{Xe}$  to  $^{140,144}\text{Xe}$ .

<sup>2</sup>The systematic uncertainty was not estimated, but will be large, because no normalisation to target excitation was possible and the analysis was done relatively to the elastic scattering.

The “safe” energy on lead is about 4.5 MeV/u ( $\vartheta_{\text{CM}} = 180^\circ$ ) applying a well-established empirical formula suited for such heavy scattering systems [29].

Scattered beam-like particles and recoiling target-like particles are kinematically well separated following simulations which take into account the energy loss in the target (interpolated using some nodes calculated with SRIM2008 [30]) and the pulse height deficit (using the simple model from Ref. [31], neglecting the small detector-dependent term).

Gamma-rays will be detected by MINIBALL [32] and the coincident particles, scattered projectiles and recoiling target nuclei, by either the CD only or by C-REX, both arrays of Si detectors. C-REX (for details see Ref. [18]) is a version of T-REX [33], optimised to perform Coulomb excitation experiments with a large angular coverage: a forward CD<sup>3</sup> ( $22^\circ < \vartheta_{\text{Lab}} < 60^\circ$ ), and in backward direction a barrel detector and a backward CD (combined  $105^\circ < \vartheta_{\text{Lab}} < 172^\circ$ ). The shift of the actual beam spot away from the centre of the set-up will be determined from elastic scattering and considered in the analysis.

Our main observable, the excitation cross section for Coulomb excitation depends not only on the transitional but also on the diagonal matrix elements (electric quadrupole moments  $Q_2$ ), an effect known as reorientation. As both the relative importance of single- and multi-step processes and the reorientation effect depend on the scattering angle, a data set with a large coverage of scattering angles in the CM system is mandatory. In the analysis, the data set is split in different angular bins. The matrix elements are then determined by a maximum likelihood fit.

At REX-ISOLDE, lower beam energies only allowed for targets with lower  $Z$ . The analysis showed that the sensitivity on multiple-step excitation processes including the reorientation was limited. Further constraints from the lifetimes were not sufficient to improve the obtained results. IS548 has demonstrated that energies at HIE-ISOLDE and high- $Z$  targets significantly improve the quantity, but also the quality, of the obtained data.

Generally, C-REX offers a more comprehensive data set, but as discussed in the following, for the proposed experiments the CD detector alone is sufficient (covered angular range  $30^\circ \lesssim \theta_{\text{CM}} \lesssim 150^\circ$ ). For both cases, the small statistics from the backwards hemisphere would not be essential for the analysis as it was the case for IS548.

For  $^{140}\text{Xe}$ , the level scheme is much better known compared to  $^{142}\text{Xe}$  and the proposed experiment aims at the determination of the electromagnetic matrix elements. Only the  $2_\gamma^+$  state and the  $4_\gamma^+$  state are unknown. These will be readily populated as demonstrated for  $^{142}\text{Xe}$ . We intend to use a  $^{208}\text{Pb}$  target. The analysis will be performed relatively to the experimental  $B(E2, 0_{gs}^+ \rightarrow 2_1^+)$  of  $^{140}\text{Xe}$  which is very well known from lifetime measurements [4, 5]. Excited states in  $^{208}\text{Pb}$  are at high excitation energy and will be only weakly excited. The respective  $\gamma$ -rays do not affect the measured spectra. As seen in Fig. 2, newly discovered transitions in the region 750-850 keV were on top of the wrongly Doppler corrected transitions from the  $^{206}\text{Pb}$  target which resulted in larger uncertainties when subtracting the background. This will be avoided by the use of the  $^{208}\text{Pb}$  target.

For  $^{144}\text{Xe}$ , this approach is not possible and an analysis relative to the target excitation is mandatory. Given the smaller beam intensity, we expect mainly the excitation of the yrast band. As in IS548, a  $^{206}\text{Pb}$  target will be used. Its  $\gamma$  ray does not interfere with the known transitions within the yrast band of  $^{144}\text{Xe}$ . If new transitions observed in  $^{144}\text{Xe}$  overlap with the  $\gamma$  ray from  $^{206}\text{Pb}$ , optional targets of  $^{204}\text{Pb}$  and/or  $^{207}\text{Pb}$  will be prepared.

In IS548 we have demonstrated that beam intensities can be consistently deduced from the

---

<sup>3</sup>The distance between forward CD and target is adjustable if more forward coverage is desired.

elastic scattering as well as from the Coulomb excitation of the first  $2^+$  state in  $^{206}\text{Pb}$ . The latter confirms that the *absolute efficiency of MINIBALL* and the  *$\gamma$ -particle coincidence efficiency* are correctly known.

Xenon beams are pure beams at ISOLDE. The only isobaric contaminants are the decay products of the Xe isotopes within the EBIS. In IS548, the daughter  $^{142}\text{Cs}$  and granddaughter  $^{142}\text{Ba}$  of  $^{142}\text{Xe}$  ( $T_{1/2} = 1.23$  s) have been observed. E.g., in Fig. 2 the  $2_1^+ \rightarrow 0_{\text{gs}}^+$  transition at 359.6 keV originating from the Coulomb excitation of  $^{142}\text{Ba}$  is clearly visible with the expected intensity. The beam intensity of  $^{142}\text{Ba}$  was consistent with the numerical solution of the Bateman equation for in-EBIS decay of  $^{142}\text{Xe}$ .  $^{140}\text{Xe}$  has a half-life of 13.6 s [34], hence there will be only a very small contribution from  $^{140}\text{Cs}$ . The half-life of  $^{144}\text{Xe}$  ( $T_{1/2} = 1.15$  s [34]) is very similar to that of  $^{142}\text{Xe}$ , hence the isobaric contaminants will have the same intensities.

The large statistics will also allow for a determination of the  $g$  factors applying the RIV method [35, 36]. Only for the  $2_1^+$  states of  $^{140,142}\text{Xe}$   $g$  factors are known [37] which had to be corrected as the lifetimes used in the original analysis were incorrect [4, 5]. Theoretical predictions are in any case much smaller than the experimental values. From our experience at REX-ISOLDE, the angular  $\gamma$ -particle correlations are already quite smoothed by the deorientation effect for lifetimes of about 100 ps, e.g., the  $2^+$  state in  $^{140}\text{Xe}$  for which we had the highest statistics. The states above have much shorter lifetimes which helps such an analysis. However, this analysis has not been done yet for the IS548 data ... the next step in our analysis.

The amount of information on the evolution of quadrupole and octupole collectivity in this region accessible by our approach cannot be obtained by other methods. Beams of neutron-rich Xe isotopes at safe energies are not available anywhere else. For short-lived states,  $Q_2$  values are only accessible by safe Coulomb excitation. Lifetime measurements do not allow for the determination of  $Q_2$  values at all, in most cases  $B(E3)$  values cannot be extracted and the sign of the matrix elements cannot be deduced. The low-lying states apart from the ground-state band could not be investigated in prompt spectroscopy of fission fragments [5, 38, 39] because they are not populated. Xe isotopes have not been studied in Coulomb excitation at intermediate beam energies, but other analyses, e.g., for  $^{136}\text{Te}$  at RIKEN [40], showed that the analysis is more difficult than previously done. But more important, the excitation of states with  $I > 2$  are very suppressed.

### 3 Rate estimate and beam time request

The Xe isotopes of interest are produced using a standard  $\text{UC}_x/\text{graphite}$  target irradiated with the proton beam from the PS Booster. The use of the VD7 ion source has been recommended [42]. As Xe is a noble gas, a cold transfer line will be used. Back in 2012 [15], a yield of  $3.7 \cdot 10^7/\mu\text{C}$  [41] was expected which would have resulted in a beam intensity around  $3.7 \cdot 10^6/\text{s}$  assuming a proton current of  $2 \mu\text{A}$  and an efficiency of HIE-ISOLDE of 5 %. The beam rate for  $^{142}\text{Xe}$  in 2016 was  $1.2 \cdot 10^5/\text{s}$ , hence an order of magnitude lower than expected, but roughly consistent with the more recent lower yield reported in Table 1. The lower yield is presumably due to the now recommended lower target temperature which was used in 2016 to enable a stable operation for a longer run [42].

Isotope	Yield ( $/\mu\text{C}$ )	Requested shifts (8h)
$^{140}\text{Xe}$	$8 \cdot 10^7$	15
$^{142}\text{Xe}$	$2 - 7 \cdot 10^6$	/
$^{144}\text{Xe}$	(protons on target) $1.8 \cdot 10^5$	4
$^{144}\text{Xe}$	(protons on converter) $9.4 \cdot 10^4$	/

Table 1: Priv. communication by S. Rothe (ISOLDE-TISD).

The expected statistics and quality of data can be scaled from the experience obtained in IS548. Especially for  $^{140}\text{Xe}$  we expect very similar  $B(E2)$  and  $B(E3)$  values as for  $^{142}\text{Xe}$ . The clear aim for  $^{140}\text{Xe}$  is an increase in statistics as compared to  $^{142}\text{Xe}$  to obtain smaller statistical errors. The beam intensity will be at least a factor of 10 higher compared to  $^{142}\text{Xe}$  (see Table 1). We intend to use a thinner target than the  $4 \text{ mg/cm}^2$  target which was used in IS548 to partially compensate for the lower than expected beam intensity. This target had considerable drawbacks due to the blur of the particle energies: (a) worse Doppler correction of the  $\gamma$  rays, (b) worse kinematical separation between projectile and target in the forward CD and (c) an increased systematical error as the excitation probabilities depend on the beam energy. With a  $2 \text{ mg/cm}^2$  target and **15 shifts** a spectrum can be obtained similar to that in Fig. 2, but with five times more statistics, no target excitation, and a better resolution. Compared to the results for  $^{142}\text{Xe}$ , this will reduce the statistical error by more than a factor of 2 and, in addition, result in an improvement of the systematical error.

For  $^{144}\text{Xe}$ , the beam intensity is by at least a factor of 10 smaller compared to  $^{142}\text{Xe}$  (see Table 1). We would like to have a (nearly) first glance on this isotope by Coulomb excitation and obtain  $B(E2)$  and  $Q_2$  values along the yrast band. The spectrum in the region 200-600 keV is very clean (see Fig. 2), therefore the use of the  $4 \text{ mg/cm}^2$  target is still appropriate. Within **3 shifts** the collected statistics will be about 1/30 compared to what is shown in Fig. 2 ... hence still more than 100 counts (particle- $\gamma$  coincidences) in the  $6_1^+ \rightarrow 4_1^+$  transition for which no counts at all were seen at REX-ISOLDE. To verify whether new transitions from  $^{144}\text{Xe}$  are hidden below transitions from the target, we will measure as first step for **1 shift** with a Mo target and “unsafe” conditions as was done, e.g., in the recent studies of Ra and Rn isotopes [43, 44]. For the  $2^+$  and  $4^+$  states the statistics is still sufficient to be split into 3-4 angular bins with below 5% statistical uncertainty each aiming for an extraction of the quadrupole moments  $Q_2$ . Scaling from  $^{142}\text{Xe}$ , also transitions from the unknown  $2_\gamma^+$  state should be seen as the total population of that state is of the same order of magnitude as for the  $6_1^+$  state. These results will contribute to the overall picture of the quadrupole collectivity in this region and will serve as base to prepare an Addendum to study this isotope more in detail.

**We ask 15+4 shifts for the study of  $^{140,144}\text{Xe}$ .**

## References

- [1] I. Arcavi et al., Nature 551, 64 (2017); M. R. Drout et al., Science 10.1126/science.aag0049 (2017); many more.
- [2] T. Behrens, Doctoral Thesis (TU München, 2010).

- [3] C. Henrich, Master Thesis (TU Darmstadt, 2014).
- [4] A. Lindroth et al., *Phys. Rev. Lett.* 82, 4783 (1999).
- [5] S. Ilieva et al., *Phys. Rev. C* 94, 034302 (2016).
- [6] W. Urban et al., *Eur. Phys. J. A* 16, 303 (2003).
- [7] W. Urban et al., *Phys. Rev. C* 93, 034326 (2016).
- [8] Y. Huang et al., *Phys. Rev. C* 93, 064321 (2016).
- [9] H. Naidja et al., *Phys. Rev. C* 96, 034312 (2017).
- [10] A. Möller et al., *Atomic Data and Nuclear Data Tables*, 94 (2008) 758–780.
- [11] K. Kumar, *Phys. Rev. Lett.* 28, 249 (1972).
- [12] D. Cline, *Ann. Rev. Nucl. Part. Sci.* 36, 683 (1986)
- [13] B. Bucher et al., *Phys. Rev. Lett.* 116, 112503 (2016).
- [14] L. Gaffney et al., ISOLDE Workshop 2017.
- [15] Th. Kröll et al., CERN-INTC-2012-041 / INTC-P-342.
- [16] C. Henrich et al., *Act. Phys. Pol. B* 49, 529 (2018).
- [17] Th. Kröll et al., CERN-INTC-2019-011 / INTC-SR-070.
- [18] C. Henrich, Doctoral Thesis (TU Darmstadt, 2021).
- [19] C. Henrich, ISOLDE News Letter 2021.
- [20] A. Yagi et al., *Accel. Prog. Rep.* 49 (2016).
- [21] S. Raman et al., *Phys. Rev. C* 43, 556 (1991).
- [22] H. Naïdja, priv. communication.
- [23] T. R. Rodríguez, priv. communication.
- [24] S. Sarkar and M. Saha Sarkar, *Phys. Rev. C* 78, 024308 (2008).
- [25] M. P. Kartamyshev et al., *Phys. Rev. C* 76, 024313 (2007).
- [26] A. Covello et al., *J. Phys.: Conf. Ser.* 267, 012019 (2011).
- [27] J. D. Holt et al., *J. Phys. G: Nucl. Part. Phys.* 39, 085111 (2012).
- [28] S. Sarkar and M. Saha Sarkar, *J. Phys.: Conf. Ser.* 267, 012040 (2011).
- [29] H. J. Wollersheim, *Habilitation Treatise* (Universität Frankfurt/M, 1993).
- [30] J. F. Ziegler, <http://www.srim.org>



- [31] G. Pasquali et al., Nucl. Instr. Meth. A 405, 39 (1998).
- [32] N. Warr et al., Eur. Phys. J. A 49, 40 (2013).
- [33] V. Bildstein et al., Eur. Phys. J. A 48, 85 (2012).
- [34] <http://www.nndc.bnl.gov>.
- [35] N. J. Stone et al., Phys. Rev. Lett. 94, 192501 (2005).
- [36] A. E. Stuchberry et al., Phys. Rev. C 96, 014321 (2017).
- [37] C. Goodin et al., Phys. Rev. C 79, 034316 (2009).
- [38] K. Kohn, Bachelor Thesis (TU Darmstadt, 2016).
- [39] G. Fernández Martínez, Doctoral Thesis (TU Darmstadt, 2018)
- [40] V. Vaquero et al. Phys. Rev. C 99, 034306 (2019).
- [41] U. C. Bergmann et al., Nucl. Instr. Meth. B 204, 220 (2003).
- [42] TAC comments for Status Report [17].
- [43] P. Butler et al., Nature Communications (2019) 10:2473.
- [44] P. Butler et al., Phys. Rev. Lett. 124, 042503 (2020).

# Appendix

## DESCRIPTION OF THE PROPOSED EXPERIMENT

The experimental setup comprises: (*name the fixed-ISOLDE installations, as well as flexible elements of the experiment*)

Part of the (if relevant, name fixed ISOLDE installation: MINIBALL + only CD, MINIBALL + T-REX)	Availability <input checked="" type="checkbox"/> Existing	Design and manufacturing <input checked="" type="checkbox"/> To be used without any modification
[Part 1 of experiment/ equipment]	<input checked="" type="checkbox"/> Existing	<input checked="" type="checkbox"/> To be used without any modification <input type="checkbox"/> To be modified
	<input type="checkbox"/> New	<input type="checkbox"/> Standard equipment supplied by a manufacturer <input type="checkbox"/> CERN/collaboration responsible for the design and/or manufacturing
[Part 2 of experiment/ equipment]	<input type="checkbox"/> Existing	<input type="checkbox"/> To be used without any modification <input type="checkbox"/> To be modified
	<input type="checkbox"/> New	<input type="checkbox"/> Standard equipment supplied by a manufacturer <input type="checkbox"/> CERN/collaboration responsible for the design and/or manufacturing
[insert lines if needed]		

HAZARDS GENERATED BY THE EXPERIMENT (if using fixed installation:) Hazards named in the document relevant for the fixed [MINIBALL + only CD, MINIBALL + T-REX] installation.

Additional hazards:

Hazards	[Part 1 of experiment/ equipment]	[Part 2 of experiment/ equipment]	[Part 3 of experiment/ equipment]
<b>Thermodynamic and fluidic</b>			
Pressure	[pressure][Bar], [volume][l]		
Vacuum			
Temperature	[temperature] [K]		
Heat transfer			
Thermal properties of materials			
Cryogenic fluid	[fluid], [pressure][Bar], [volume][l]		
<b>Electrical and electromagnetic</b>			
Electricity	[voltage] [V], [current][A]		
Static electricity			
Magnetic field	[magnetic field] [T]		
Batteries	<input type="checkbox"/>		

Capacitors	<input type="checkbox"/>		
<b>Ionizing radiation</b>			
Target material [material]			
Beam particle type (e, p, ions, etc)			
Beam intensity			
Beam energy			
Cooling liquids	[liquid]		
Gases	[gas]		
Calibration sources:	<input type="checkbox"/>		
• Open source	<input type="checkbox"/>		
• Sealed source	<input type="checkbox"/> [ISO standard]		
• Isotope			
• Activity			
Use of activated material:			
• Description	<input type="checkbox"/>		
• Dose rate on contact and in 10 cm distance	[dose][mSV]		
• Isotope			
• Activity			
<b>Non-ionizing radiation</b>			
Laser			
UV light			
Microwaves (300MHz-30 GHz)			
Radiofrequency (1-300 MHz)			
<b>Chemical</b>			
Toxic	[chemical agent], [quantity]		
Harmful	[chem. agent], [quant.]		
CMR (carcinogens, mutagens and substances toxic to reproduction)	[chem. agent], [quant.]		
Corrosive	[chem. agent], [quant.]		
Irritant	[chem. agent], [quant.]		
Flammable	[chem. agent], [quant.]		
Oxidizing	[chem. agent], [quant.]		
Explosiveness	[chem. agent], [quant.]		
Asphyxiant	[chem. agent], [quant.]		
Dangerous for the environment	[chem. agent], [quant.]		
<b>Mechanical</b>			

Physical impact or mechanical energy (moving parts)	[location]		
Mechanical properties (Sharp, rough, slippery)	[location]		
Vibration	[location]		
Vehicles and Means of Transport	[location]		
<b>Noise</b>			
Frequency	[frequency],[Hz]		
Intensity			
<b>Physical</b>			
Confined spaces	[location]		
High workplaces	[location]		
Access to high workplaces	[location]		
Obstructions in passageways	[location]		
Manual handling	[location]		
Poor ergonomics	[location]		

Hazard identification:

Average electrical power requirements (excluding fixed ISOLDE-installation mentioned above): [make a rough estimate of the total power consumption of the additional equipment used in the experiment]: ... kW